

# Bed Load Influence on Scour at Submerged Weirs

Dawei Guan

*PhD student, Dept. of Civil and Environmental Engineering, The University of Auckland, Auckland, 1142, New Zealand. Email: dgua324@aucklanduni.ac.nz*

Bruce Melville

*Professor, Dept. of Civil and Environmental Engineering, The University of Auckland, Auckland, 1142, New Zealand. Email: b.melville@auckland.ac.nz*

Heide Friedrich

*Lecturer, Dept. of Civil and Environmental Engineering, The University of Auckland, Auckland, 1142, New Zealand. Email: h.friedrich@auckland.ac.nz*

**ABSTRACT:** Submerged weirs or sills are low head hydraulic structures that span the full width of the channel for limiting excessive bed degradation and for bed stabilization. However, in alluvial rivers their presence in the flow also results in a local scour phenomenon which may undermine the structures themselves. This paper presents an experimental study on the influence of bedload transport on the scouring process at submerged weirs under live-bed conditions. Different flow rates and weir heights were applied to the tests in this study. Bed profile measurements along the flume were recorded as a function of time using Seatek's Multiple Transducer Arrays (MTAs). Under live-bed scour conditions, scour downstream of submerged weirs develops very fast. The maximum scour depth downstream of the weir is attained within a very short time then fluctuates around a mean depth in response to migrating bed forms. The magnitude and frequency of fluctuations is strongly dependent on the bed features (patterns and transport rates) that propagate through the scour zone. Observations show a scour and fill process occurring immediately upstream of the weir. The scour hole at the upstream base of the weir develops as a dune trough approaches the weir, and reaches its maximum size when the dune trough arrives at the weir, then gradually fills as the next dune crest arrives. A prediction equation is proposed for scour at submerged weirs under live-bed scour conditions.

**KEY WORDS:** Scour, Submerged weir, Bedload, Live-bed conditions, Bedforms

## 1 INTRODUCTION

Scouring typically occurs around hydraulic structures in streams and rivers with erodible beds as a result of flow disturbance. Submerged weirs or sills are low head hydraulic structures that span the full width of the channel for limiting excessive bed degradation and for bed stabilization, raising upstream water level and reducing flow velocity. However, in alluvial rivers their presence in the flow also results in a local scour phenomenon, which may undermine the structures themselves. The subject of scour downstream of bed sills has been extensively studied, and many scour prediction equations have been published (Bormann and Julien 1991, Gaudio et al. 2000, Lenzi et al. 2003, D'Agostino and Ferro 2004, Ben Meftah and Mossa 2006, Marion et al. 2006). However, all these studies have ignored the influence of the propagation of upstream bedforms over the weir, which is likely to occur in alluvial rivers during flood events. A sketch of scour at a submerged weir under live-bed scour conditions is shown Figure 1.

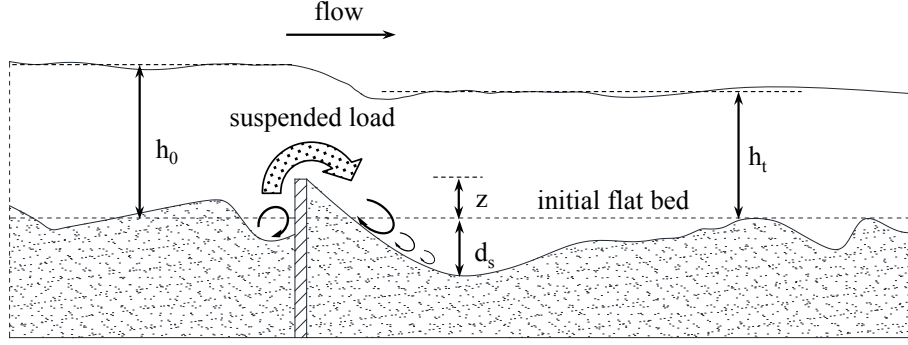


**Figure 1** Sketch of scour at a submerged weir under live-bed scour conditions

Based on the concepts of jet diffusion and particle stability in scour holes, Bormann and Julien(1991) carried out a large-scale physical model study on scour downstream of partially submerged weirs. They considered a wide range of configurations (jet angles, flow submergence, face angles of the weir) under clear water scour conditions. Their equation for estimating equilibrium scour depth downstream of the weir has the following form:

$$d_s = \frac{Kq^{0.6}U_w \sin \beta}{g^{0.8}d_{90}^{0.4}} - z \quad (1)$$

where  $d_s$  is maximum scour depth downstream of the weir;  $K$  is a coefficient depending on jet configuration, inlet geometry and sediment properties;  $q$  is unit discharge;  $U_w$  is average velocity at the weir crest;  $\beta$  is upstream face angle of the scour hole;  $g$  is gravity acceleration;  $d_x$  is sediment size for which  $X\%$  of particles are finer; and  $z$  is weir height above original bed level.

For estimations of upstream face angle of the scour hole  $\beta$  and coefficient  $K$ , Bormann and Julien (1991) proposed the following equations:

$$\beta = 0.316 \sin \lambda + 0.15 \ln \left( \frac{h_0}{h_0 - z} \right) + 0.13 \ln \left( \frac{h_t}{h_0 - z} \right) - 0.05 \ln \left( \frac{U_w}{\sqrt{g(h_0 - z)}} \right) \quad (2)$$

$$K = C_d^2 \left\{ \rho \sin \varphi / [\sin(\varphi + \beta) C_f (\rho_s - \rho)] \right\}^{0.8} \quad (3)$$

where  $\lambda$  is face angle of the weir;  $h_0$  is approach flow depth;  $h_t$  is tailwater depth;  $C_d$  is jet diffusion coefficient (taken as 1.8);  $C_f$  is coefficient of friction relationship (taken as 2.0);  $\varphi$  is submerged repose angle of sediment; and  $\rho$  and  $\rho_s$  are density of water and sediment, respectively.

D'Agostino and Ferro (2004) described an approach for predicting local scour downstream of weirs. Applying the incomplete self-similarity theory to dimensionless groups and combining it with a multiple regression of numerous data from published papers and experiments, they obtained the following equation:

$$\frac{d_s}{z} = 0.540 \left( \frac{b}{z} \right)^{0.593} \left( \frac{h_t}{H_d} \right)^{-0.126} \left( \frac{Q}{bz\sqrt{gd_{50}(\rho_s/\rho - 1)}} \right)^{0.544} \left( \frac{d_{90}}{d_{50}} \right)^{-0.856} \left( \frac{b}{B} \right)^{-0.751} \quad (4)$$

where  $H_d$  is head drop across the structure;  $b$  is weir width;  $B$  is channel width;  $Q$  is discharge. It is clear that Equation (4) is applicable to the non-uniform sediment condition, different structure patterns (structure height and width) and different channel geometries (channel width). Using a methodology similar to that of D'Agostino and Ferro (2004), Scurlock et al. (2011) produced specific equations with the same form as Equation (4) for the three-dimensional weirs (-U, -A, -W). However, all their tests were confined to clear water scour conditions and had a relatively large head drop ( $h_0 - h_t$ ) at the weir.

Marion et al. (2006) were the first investigators to evaluate the effect of upstream sediment supply on scour depth and shape downstream of a sequence of bed sills. Based on dimensional analysis, existing

experimental data sets (Gaudio et al. 2000, Lenzi et al. 2002, Gaudio 2003, Lenzi et al. 2003, Marion et al. 2004) and a new set of experiments, Marion et al. (2006) derived the following equation for the prediction of the maximum scour hole depth:

$$\frac{d_s}{H_s} = 3.0 \left( \frac{a_l}{H_s} \right)^{0.60} SI^{-0.19} \left( 1 - e^{-0.25 \frac{L}{H_s}} \right) \quad (5)$$

where  $H_s$  is critical specific energy;  $a_l$  is the morphological jump, defined as the difference between initial and final slope multiplied by the length between structures;  $SI$  is sediment sorting index, calculated as  $0.5(d_{84}/d_{50} + d_{50}/d_{16})$ ; and  $L$  is the length between structures. Because a wide range of data were used in this calibration, Equation (5) is applicable for  $0.07 \leq a_l/H_s \leq 1.87$ , and should be applicable to various conditions: high and low bed slopes, uniform and mixed grain sizes, and clear water and live-bed conditions (with steady sediment feeding rate). This study is significant due to its consideration of the effect of upstream sediment supply, which considerably reduced the scour hole dimensions downstream of the weir when compared with clear water experiments. However, the sediment particles they used in all the tests were gravel (for no sediment supply tests,  $d_{50} = 1.8\text{mm}$  to  $8.7\text{mm}$ ; for sediment supply tests,  $d_{50} = 8.7\text{mm}$ ) and their study was restricted to only mountain rivers that have relatively large slopes. Therefore, the applicability of Equation (5) to the scour case that occurs in alluvial rivers with bedform propagation needs to be validated.

Another similar dimensional analysis methodology is that of Ben Meftah and Mossa (2006), who proposed that:

$$\frac{d_s}{H_s} = 0.59 \frac{\Delta LS}{H_s} + 1.74 \quad (6)$$

where  $S$  is initial bed slope. Equation (6) is only applicable to uniform sediment size ( $d_{50} = 1.8\text{mm}$ ) and clear water scour conditions.

Almost all the data used in the derivation of Equations (1) to (7) were obtained under clear water scour conditions. No observations were made in conditions of bed propagation over a submerged weir, conditions which occur in alluvial rivers during high flows. Therefore, the aims of this experimental study are to understand bedload influence on scour at submerged weirs and to develop a predictive equation for the maximum scour depth downstream of submerged weirs under live-bed conditions.

## 2 EXPERIMENTAL SET-UP AND PROCEDURE

The experiments were conducted in a tilting flume, 12m long, 0.44m wide and 0.38m deep, in the Hydraulic Laboratory of The University of Auckland. The flume has two pumps for recirculating both sediment and water. The speed of the main pump was controlled by a variable speed electronic control unit while the sediment pump speed was set to constant speed that gave adequate capacity. At the upstream end of the flume, water and sediment are fed into a mixing chamber and enter the flume through a honeycomb flow straightener which effectively eliminates any rotational flow component induced in the return pipelines. At the downstream end, bedload sediment is trapped in a separate hopper-like sump and pumped to the inlet by the sediment pump; water and little suspended sediment are pumped with either or both water pumps.

The sediment used in the experiments was coarse sand, with the median diameter,  $d_{50} = 0.85\text{mm}$  and relative submerged particle density  $\Delta = 1.65$ . The sediment size distribution was near uniform with a standard deviation  $\sigma_g = 1.3$ . The weirs used in experiments were 1 mm-thick rectangular plastic plates, with the same width as the flume.

The three-dimensional scour geometry downstream of the weir was measured as a function of time throughout the experiment using Seatek's Multiple Transducer Arrays (MTAs). The instrument is an ultrasonic ranging system, comprising 32 transducers, which can detect the distance from the sensors to reflective objects. The system was operated at 5Hz with 25 transducers and the measuring accuracy of the system is approximately  $\pm 1$  mm. A detailed description of this device was given by Friedrich et al. (2005). The transducers were mounted in a rectangular grid on a carriage that can be moved along the top rail of the flume. To avoid interference with bed profile measurements by reflections from the suspended

sediment particles, the average approach velocities were temporarily reduced to values that were below the critical average velocities in live-bed scour tests. It was assumed that temporarily reducing flow rates for the collection of topographic data would have minimal effects on reshaping of the bedform features and the scour geometries. The assumption was validated because the observed slope angles of bedforms and scour geometries were smaller than the sediment submerged repose angle in all the tests. The same assumption was made by Scurlock(2011) for topographic measurements after draining the flume. After each bed profile measurement, maximum scour depth,  $d_s$ , downstream of the weir and its location were found on the contour plots using a compiled Matlab programme. An example of a processed bed profile is shown in Figure 2. For the live-bed scour tests, scour depth at the upstream base of the weir and the bed elevation change upstream of the weir were measured with two additional transducers.

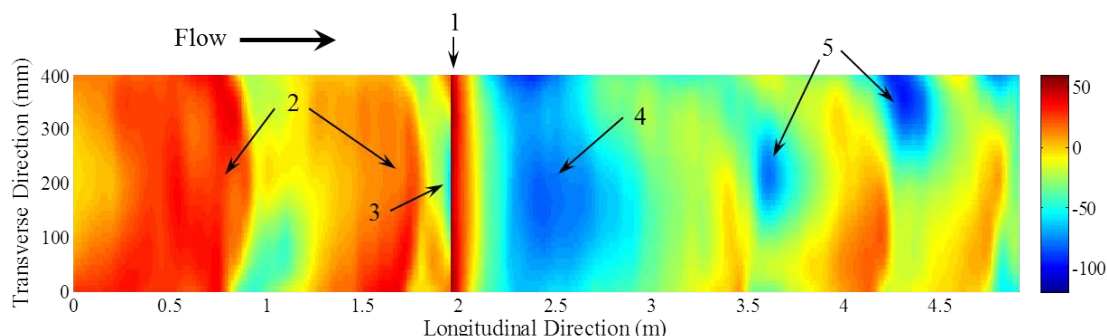


**Figure 2** Bed profile at  $t = 150$  min in test NLS21, contours in mm; 1- submerged weir, 2- approaching dunes, 3- upstream scour hole, 4- downstream scour hole, 5- downstream migrating scour holes

Five clear water scour tests and nine live-bed scour tests were carried out. For each weir height tested, the flow rate,  $Q$ , was systematically varied and the tailwater depth,  $h_t$ , was adjusted to normal depth at the beginning of the test by adjusting the flume slope and the overflow pipe in the sump at the end of the flume. The water surface profiles were measured using a point gage to determine the water level change across the weir and the average approach flow depth,  $h_0$ . The experimental conditions and results are shown in Table 1.

**Table 1** Experimental conditions and results

Test	$Q$ ( $m^3/s$ )	$z$ (mm)	$H_d$ (mm)	$h_t$ (mm)	$h_0$ (mm)	$U_0$ (m/s)	$U_c$ (m/s)	$d_{se}$	$t$ (hours)
CS1	0.018	40	- <sup>a</sup>	150	150	0.266	0.367	101 <sup>b</sup>	118
CS2	0.020	40	- <sup>a</sup>	150	150	0.296	0.367	151.2	533.5
CS3	0.021	40	- <sup>a</sup>	150	150	0.313	0.367	167.8 <sup>b</sup>	102.5
CS4	0.022	30	- <sup>a</sup>	150	150	0.333	0.367	135 <sup>b</sup>	94
CS5	0.021	50	- <sup>a</sup>	150	150	0.314	0.367	199 <sup>b</sup>	97.5
NLS3	0.038	40	10	145	155	0.553	0.368	80.6	44.5
NLS5	0.049	40	16	145	161	0.687	0.370	86.4	41.5
NLS7	0.059	40	28	145	173	0.772	0.374	116.3	23
NLS11	0.035	30	7	145	152	0.517	0.367	57.1	23
NLS13	0.050	30	13	145	158	0.724	0.369	67.7	23
NLS15	0.058	30	17	145	162	0.819	0.371	91.25	24
NLS19	0.035	50	16	145	161	0.492	0.370	83	23.5
NLS21	0.047	50	27	145	172	0.621	0.374	103	23
NLS23	0.058	50	38	145	183	0.723	0.377	138.5	24

<sup>a</sup>: no obvious head drop  $H_d$  was observed;  
<sup>b</sup>: extrapolated values

### 3 RESULTS AND DISCUSSION

#### 3.1 Scour mechanics

For the clear water scour, the equilibrium of the scour process is defined as the condition when the dimensions of the scour hole do not grow with time. It may take several days or weeks to attain equilibrium conditions even in small scale laboratory tests (Melville and Chiew 1999). Figure 3a shows the temporal development of maximum scour depth downstream of the weir. The trends clearly show three stages: 1) initial fast stage; 2) progressing stage; 3) equilibrium stage. It can be seen that only test CS2 achieved the equilibrium condition and the temporal evolution curves for the other four clear water scour tests were extrapolated to the final scour depth. The fitting process of the experimental data was done using the expression  $d_s(t) = a \exp\{-b[\ln(t/c)]^d\}$ , where  $a$ ,  $b$ ,  $c$  and  $d$  are fitting coefficients. This expression is based on the time scale for clear water scour at piers (Melville and Chiew 1999). Curve extrapolation was based on the curvature of existing data and the trend of test CS2. Although extrapolated values were obtained with much caution, the process may incur errors in the equilibrium scour depth. The main purpose of obtaining final scour depth for clear water scour tests is to provide a comparison for the live-bed scour test results.

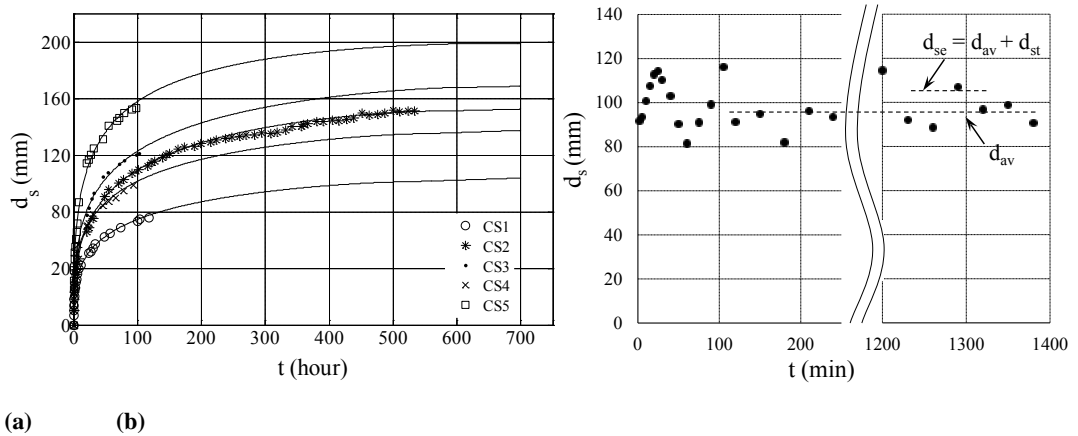


**Figure 3** Temporal development of downstream maximum scour depth: (a) clear water scour tests, (b) live-bed scour test NLS21

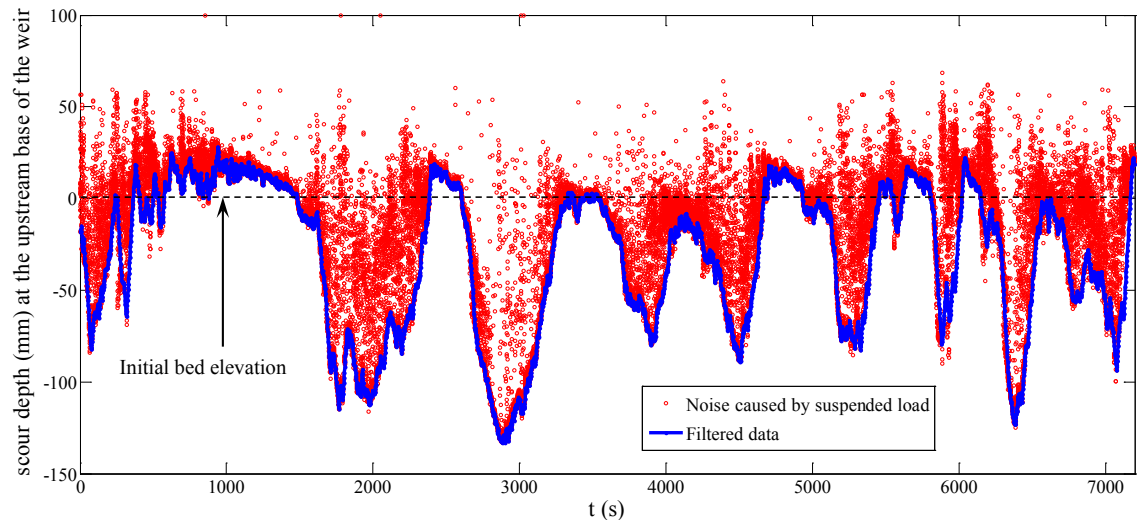
For the live-bed scour, bed scour occurs both upstream and downstream of the weir, and sediment transport processes are highly influenced by strong turbulence created by the submerged weir. At the weir, the approach flow is accelerated at the crest of the weir and a back flow is created immediately upstream of the weir. Sediment transport over the weir occurs as suspended load, with entrainment by the strongly accelerating flow on the crest of the weir. The impinging flow immediately downstream of the weir greatly increases the flow turbulence intensities and creates a big scour hole. Near the weir and in the scour holes, sediment moved both as suspended load and bed load.

The maximum scour depth downstream of the weir was attained within a very short time then fluctuated around a mean depth,  $d_{av}$ , in response to the migrating bed forms (Figure 3b). The magnitude and frequency of fluctuations is strongly dependent on the bed features (patterns and transport rate) that propagate through the scour zone. Although the structure itself and flow over the structure were two dimensional, the scour hole downstream of the submerged weir presented three dimensional characteristics due to the three-dimensional migrating bed features. The locations of the fluctuating maximum scour depth were found frequently to “drift” near side walls both in clear water scour and live-bed scour tests, indicating strong secondary currents formed in the scour holes downstream of the weir.

In this study, the equilibrium scour depth,  $d_{se}$ , is calculated as the summation of the mean maximum scour depth,  $d_{av}$ , and the standard deviation of maximum scour depths,  $d_{st}$  (Figure 3b). A scour and fill process occurred immediately upstream of the weir. Figure 4 shows an example of the scour evolution at the upstream base of the weir. The measurement point was set on the centreline of the flume and 15mm from the upstream face of the weir. The scour hole at the upstream base of the weir develops as a dune

trough approaches the weir, and reaches its maximum size when the dune trough arrives at the weir, then gradually fills as the next dune crest arrives (see Figure 2). As the flow passes a dune crest, a flow separation zone forms on the leeside of the dune. Associated with the separation zone is a turbulent free shear layer generating large scale eddies that travel through the flow domain and toward the surface while dissipating (Stoesser et al. 2008). Therefore, it can be inferred that periodic interactions between this flow structure in the dune trough and the back flow at the upstream base of the weir result in a scour and fill process occurring immediately upstream of the weir. Because insufficient experimental data were recorded, the magnitude of the scour depth upstream of the weir is not discussed here.

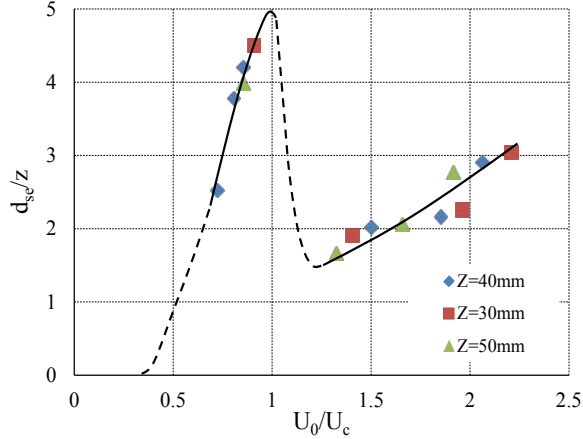
During live-bed scour tests, migrating scour holes downstream of the first scour hole after the weir were observed (see Figure 2). It was inferred that these migrating scour holes result from migrating dunes propagating over the scour zone downstream of the weir. The longitudinal distance between two adjacent migrating scour holes is approximately the same as that of two adjacent approaching dune troughs in the upstream reach (Figure 2).



**Figure 4** Scour process at the upstream base of the weir; test NLS 13 (5Hz, 36000 samples)

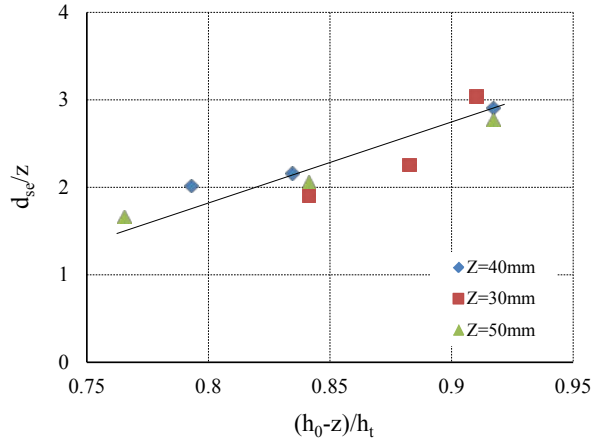
### 3.2 Effect of flow intensity and water level change across the weir

Figure 5 shows the normalized values of the equilibrium scour depth,  $d_{se}/z$ , downstream of the weir as a function of flow intensity  $U_o/U_c$ . The trend line shows that the equilibrium scour depth reaches its peak at the transition ( $U_o/U_c = 1$ ) from clear water scour to live-bed scour conditions, and then experiences a significant drop just beyond the peak. In both scour conditions, the equilibrium scour depth increases with the increase of the flow intensity, but at different rates. The significant drop and two different increase rates in equilibrium scour depth are a consequence of the difference between the rates of upstream sediment transport and scour hole development. For live-bed scour at piers or abutments, a similar trend occurs. Scour depth initially reduces with increase in approach flow velocity, reaches a minimum value, and then increases again toward a second maximum. The second maximum occurs at about the transitional flat-bed stage of sediment transport on the channel bed and is termed live-bed peak (Melville 1997). Although Figure 5 shows a similar trend as that of scour at piers and abutments, the live-bed peak cannot be determined from results of this study, because the transitional flat-bed stage of sediment transport was not reached.



**Figure 5** Normalized scour depth as a function of flow intensity

In live-bed conditions, the submerged weir significantly raised the water level of the approach flow. The water level change across the weir increased with increasing flowrate. An increase in the upstream water level not only affects the impinging flow angle immediately downstream of the weir, but also alters upstream bed features and bed slope. Observation shows that some aggradation occurred on the upstream bed in live-bed conditions. The normalized water level difference is calculated as the ratio of water depth above the weir crest to the normal tailwater depth (Figure 6). It can be seen in Figure 6 that the equilibrium scour depth shows an increasing trend as the water level difference across the weir increases. This is consistent with the trend of scour downstream of non-submerged drop structures, which has been well documented in the literature (Schoklitsch 1932, Bormann and Julien 1991, Hoffmans and Pilarczyk 1995, D'Agostino and Ferro 2004).



**Figure 6** Normalized scour depth as a function of normalized water level difference across the weir (live-bed conditions)

### 3.3 Prediction of equilibrium scour depth downstream of the weir with bed load influence

The geometry of the submerged weir under live-bed scour conditions has been sketched in Figure 1. The equilibrium scour depth,  $d_{es}$ , can be expressed as:

$$d_{se} = f(\rho, \nu, g, h_0, h_t, U_0, \rho_s, d_{50}, \sigma_g, U_c, b, z) \quad (7)$$

where  $\nu$  is the fluid viscosity. Equation (7) includes a consideration of approach flow and tailwater conditions ( $\rho, \nu, g, h_0, U_0, h_t$ ), sediment characteristics and transport ( $\rho_s, d_{50}, \sigma_g, U_c$ ), and structure geometry ( $b, z$ ).

In this study, the same sediment and a constant weir width have been used. Thus, assuming constant relative density of sediment and fluid viscosity, adimensionless expression for the equilibrium scour depth downstream of the submerged weir in a uniform sediment can be developed from Equation (7) as follows:

$$\frac{d_{se}}{z} = f\left(\frac{U_0}{U_c}, \frac{h_0 - z}{h_i}\right) \quad (8)$$

Based on a multiple regression of the data in Table 1, the following predictive equation is obtained:

$$\frac{d_{se}}{z} = 2.27 \left(\frac{U_0}{U_c}\right)^{0.512} \left(\frac{h_0 - z}{h_i}\right)^{1.948} \quad (9)$$

The multiple correlation coefficient  $R$  for Equation (9) is 0.963, and the mean relative deviation (MRD), which is defined as:

$$MRD = \frac{1}{n} \sum_{i=1}^n \left| \frac{d_{se,i,observed} - d_{se,i,calculated}}{d_{se,i,observed}} \right| \quad (10)$$

is calculated as 0.053. A comparison between measured equilibrium scour depth,  $d_{se}$ , and predicted values by Equations (1, 4, 5, 6, and 9) for the live-bed scour tests is shown in Figure 7. The morphological jump  $a_1$  in Equation (5) and the product “ $LS$ ” in Equation (6) are taken as the weir height  $z$  in this study.

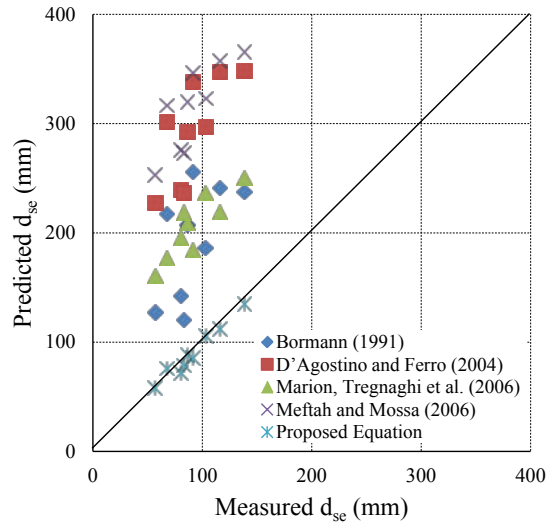


**Figure 7** Comparison between measured equilibrium scour depth and predicted values by Equations (1, 4, 5, 6, and 9) for the live-bed scour tests

As seen in Figure 7, all the equations found in the literature greatly overestimate the equilibrium scour depth downstream of the weir. One of most important reasons is that their developments excluded the upstream bedform influence. In reality, bedforms propagate over the submerged weir during high flows, and this significantly reduces the scour volume downstream of the structure. The bedload impact on scouring, identified by this study, should be considered at the structure design stage. It should be noted that Equation (9) was developed for  $U_0/U_c$  in the range 1.33-2.21. As only one size of uniform sediment was used in this study, the equation does not consider sediment size variation or gradation effects.



## 4 CONCLUSIONS

This study investigated the influence of bed load on scour at submerged weirs. The experiments are limited to rectangular weirs in uniform sand beds. Under live-bed scour conditions, a scour and fill process occurs immediately upstream of the weir, and scouring downstream of the submerged weir develops very quickly. The maximum scour depth downstream of the weir is attained within a very short time, and then fluctuates around a mean depth in response to the migrating bed forms. The relationship between the normalized equilibrium scour depth downstream of the weir ( $d_{se}/z$ ) and flow intensity ( $U_o/U_c$ ) shows that the equilibrium scour depth reaches its peak at the transition from clear water scour to live-bed scour conditions and experiences a significant drop just beyond the peak. In both scour conditions, the normalized equilibrium scour depth ( $d_{se}/z$ ) increases with increasing flow intensity, but at different rates. Under live-bed conditions, the normalized equilibrium scour depth downstream of the weir ( $d_{se}/z$ ) appears to be highly correlated with the dimensionless group  $(h_o - z)/h_t$ . A predictive equation (Equation 9) has been proposed for scour at submerged weirs under live-bed scour conditions.

## ACKNOWLEDGEMENT

The authors would like to thank China Scholarship Council (CSC) for the financial support of this research. Also, the valuable suggestions from Dr. Keith Adams are appreciated.

## References

- Ben Meftah, M., and Mossa, M., 2006. "Scour holes downstream of bed sills in low-gradient channels." *Journal of Hydraulic Research*, 44(4), 497-509.
- Bormann, N. E., and Julien, P. Y., 1991. "Scour Downstream of Grade-Control Structures." *Journal of Hydraulic Engineering*, 117(5), 579-594.
- D'Agostino, V., and Ferro, V., 2004. "Scour on Alluvial Bed Downstream of Grade-Control Structures." *Journal of Hydraulic Engineering*, 130(1), 24-37.
- Friedrich, H., Melville, B. W., Coleman, S. E., Nikora, V. I., and Clunie, T. M., 2005. "Three-dimensional measurement of laboratory submerged bed forms using moving probes." *Proc., XXXI IAHR Congress*, 396-404.
- Gaudio, R., 2003. "Time evolution of scouring downstream of bed sills." *Journal of Hydraulic Research*, 41(3), 271-284.
- Gaudio, R., Marion, A., and Bovolin, V., 2000. "Morphological effects of bed sills in degrading rivers." *Journal of Hydraulic Research*, 38(2), 89-96.
- Hoffmans, G. J. C. M., and Pilarczyk, K. W., 1995. "Local Scour Downstream of Hydraulic Structures." 121(4), 326-340.
- Lenzi, M. A., Marion, A., and Comiti, F., 2003. "Local scouring at grade-control structures in alluvial mountain rivers." *Water Resour. Res.*, 39(7), 1176.
- Lenzi, M. A., Marion, A., Comiti, F., and Gaudio, R., 2002. "Local scouring in low and high gradient streams at bed sills." *Journal of Hydraulic Research*, 40(6), 731-739.
- Marion, A., Lenzi, M. A., and Comiti, F., 2004. "Effect of sill spacing and sediment size grading on scouring at grade-control structures." *Earth Surface Processes and Landforms*, 29(8), 983-993.
- Marion, A., Tregnaghi, M., and Tait, S., 2006. "Sediment supply and local scouring at bed sills in high-gradient streams." *Water Resources Research*, 42(6), W06416.
- Melville, B., and Chiew, Y., 1999. "Time Scale for Local Scour at Bridge Piers." *Journal of Hydraulic Engineering*, 125(1), 59.
- Melville, B. W., 1997. "Pier and Abutment Scour: Integrated Approach." *Journal of Hydraulic Engineering*, 123(2), 125-136.
- Schoklitsch, A., 1932. "Kolkbildung unter Überfallstrahlen." *Die Wasserwirtschaft*, 341.
- Scurlock, S. M., Thornton, C. I., and Abt, S. R., 2011. "Equilibrium Scour Downstream of Three-Dimensional Grade-Control Structures." *Journal of Hydraulic Engineering*, 1(1), 289.
- Stoesser, T., Braun, C., García-Villalba, M., and Rodi, W., 2008. "Turbulence Structures in Flow over Two-Dimensional Dunes." *Journal of Hydraulic Engineering*, 134(1), 42-55.